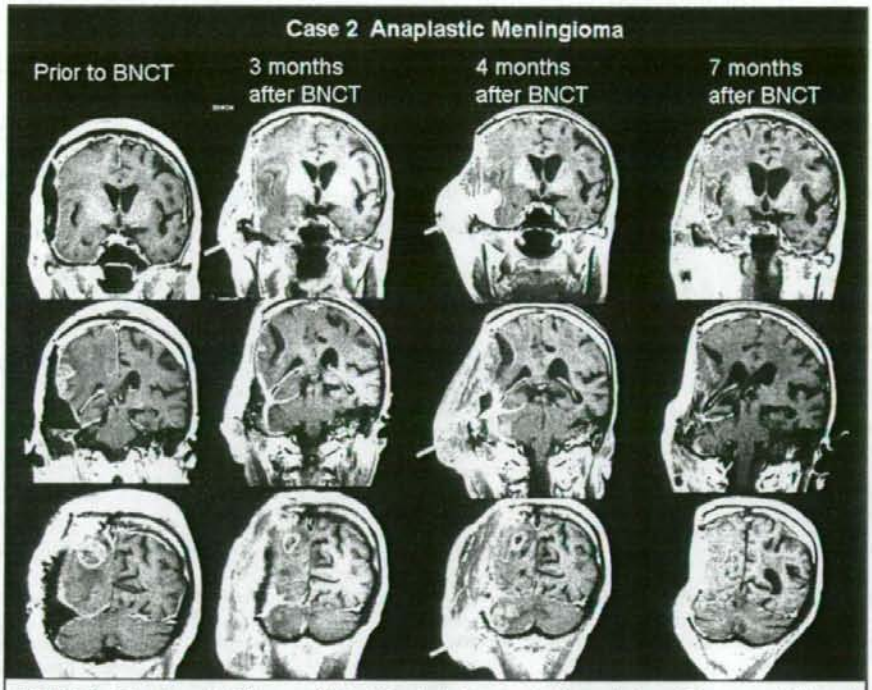

FIGURE 2. *Gd-enhanced MRI scans of Patient 2, who had an anaplastic meningioma. The upper, middle, and lower panels show the different planes of coronal sections. The right parietal, occipital masses were observed in the MRI scan just before BNCT. In addition, a small, enhanced lesion was identified on the right temporal surface. These lesions continued to shrink and eventually disappeared. A musculocutaneous flap was placed 2 months after BNCT. Three months after the first BNCT, a small subcutaneous lesion was observed which grew rapidly for only 1 month. Temporal and cerebellar lesions became obvious at 4 months after the first BNCT.* Arrows *indicate these subcutaneous meningiomas, which continued to shrink during the observation period.*

A side effect of mucositis in the oral cavity occurred with each treatment but disappeared after 2 to 3 weeks in each instance. The patient continues to do well and shows no signs of tumor regrowth (see Addendum).

Patient 5

Patient 5 was a 57-year-old woman who had undergone surgery for a right sphenoid ridge meningioma 28 years before with subtotal resection. She had also undergone three additional operations during the intervening years and had received SRS two times, 9 years and 10 months previously, with a marginal dose of 12 Gy. She experienced tumor extension in the right submandibular region, and biopsy was performed by an otorhinolaryngology team. The histological diagnosis was sarcoma, and an FDG-PET study revealed a metastasis at the right cervical lymph node. Neurosurgeons and otorhinolaryngology surgeons at the original hospital judged it impossible to control this tumor by the ordinal treatment and introduced her to our clinic. On admission to our clinic, the patient's chief complaints were right facial and neck pain. The tumor extended from the right paranasal sinuses to the cranial base, including the clivus and the cavernous sinuses on both sides on MRI scans. We decided to treat her with fractionation from both sides to achieve the putative curative dose for the midline lesion. In addition, the right cervical metastasis was treated by BNCT. The first BNCT was performed from both sides, as scheduled. At the second BNCT, which was applied 2 weeks after the first BNCT, the patient was treated from the right side. After this neutron irradiation, she began to experience high fever and chills. We, therefore, abandoned the irradiation on the left side. After the repetitive BNCTs, the tumor started to shrink, as shown in *Figure 5*. Interestingly, the lymph node metastasis also disappeared entirely in the follow-up image. The patient's neck pain and facial pain disappeared in response to the treatment. Most likely, the facial and neck pain had occurred because of trigeminal nerve compression at the cranial base and lymph node swelling, respectively. No side effects (other than mucositis in the oral cavity) or regrowth of the tumor have been observed during the observation period, whereas metastases were observed in the lungs and liver at the time of preparation of this manuscript.

Patient 6

Patient 6 was a 72-year-old woman who had undergone surgery for a falcotentorial meningioma 18 months earlier. The histological diagnosis was atypical meningioma. After the first operation, she received two courses of SRS with a marginal dose of 9 Gy and additional salvage surgery. Even with these treatments, however, the residual tumor continued to grow. She was referred to our clinic for BNCT. BPA-PET showed a relatively low T/N ratio of 2.0, and the mass size was too large for a single session of BNCT (93.7 ml). We, therefore, decided to treat her twice with BNCTs with a 2-week interval. As *Figure 6* shows, the enhanced mass was reduced somewhat after repetitive BNCTs, and the perilesional edema increased remarkably 7 weeks after the first BNCT. After discharge, the patient complained of aggravation of the visual field and consciousness disturbance. Steroids are still being administered to the patient, and her consciousness has recovered with this steroid administration (see Addendum).

DISCUSSION

The clinical features of MM include an invasive behavior and a high tendency toward recurrence, as described in this report. Only radical resection constitutes an effective landmark for good prognosis for MMs (3, 19). In general, meningiomas themselves are known to be radio-insensitive (18, 22), and the effects of radiotherapy on MMs are controversial (13). Even

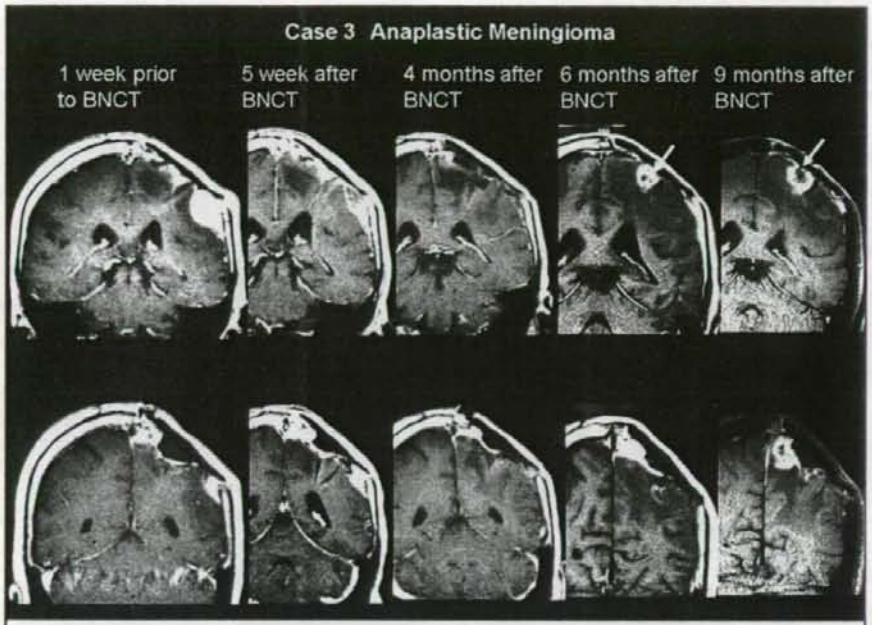

FIGURE 3. *Gd-enhanced coronal MRI scans of Patient 3, who had an anaplastic meningioma. A growing tumor was identified on the left frontoparietal convexity with subcutaneous bulging, just before BNCT. In addition, a small Gd-enhanced mass was identified close to the SSS. In the follow-up images, the main mass gradually become smaller, and it cannot be seen in the MRI scan taken 4 months after BNCT, whereas the concomitant mass close to the SSS became large after transient shrinkage. The relative volumes of the lesion close to the SSS compared with the initial volume are 122, 48.3, 75.4, and 144.2% at 5 weeks, 4 months, 6 months, and 9 months after BNCT, respectively. The arrows indicate the newly appeared lesions, which were proven to be the result of radiation necrosis on recraniotomy.*

with SRS, the 5-year survival and progression-free survival rates of MMs are only 40 and 26%, respectively (16). In addition, once the tumor has recurred, local tumor control is difficult (21). In fact, all patients in our series received repetitive surgical resections and radiotherapies during the short clinical course, even though there may have been bias in that uncontrollable cases were introduced to our institute. Strictly speaking, atypical meningiomas are not classified as MMs (12) but rather as World Health Organization Grade 2. On the other hand, sarcomas may be the most malignant form of meningiomas, as described elsewhere (20). In this study, we describe all of the tumors (World Health Organization Grades 2 and 3 and sarcomas) as malignant tumors related to meningiomas.

Rationale of PET-based BNCT for MMs

BNCT might have several advantages as a treatment for MMs. First, as described in this report, BNCT is theoretically a tumor-selective high linear energy transfer and high relative biological effect particle radiation therapeutic. It should, therefore, work better than low linear energy transfer radiation therapy using photons, even for radio-insensitive tumors such as meningiomas (11). Secondly, as Joensuu et al. (9) reported, and as we have shown here, MMs show a relatively high T/N ratio of BPA uptake by PET analysis. Third, BPA-PET is a very potent method of analysis not only for dose planning but also for decisions regarding the radiation field (6, 7). As stated in the Results section, in Patient 2, only the BPA-PET study showed a lesion of the cerebellum, whereas Gd-enhanced MRI scanning did not. This functional diagnostic tool provided us with useful information for the radiation field. In addition, cerebrospinal fluid dissemination is less frequent in MMs than in malignant gliomas, although systemic metastasis may occur, as it did in Patients 2 and 5 (4).

In preliminary reports, photon irradiation followed by proton beam irradiation has been indicated to be a promising radiation modality for MMs (5). Theoretically, proton beam irradiation has the advantage of precise dose distribution, even for irregularly shaped masses, by virtue of the Bragg peak. However, even with conformal proton beam radiation, the treatment of patients with lesions very close to the skin, such as in Patients 1, 2 (subcutaneous lesion), 3, and 5, is problematic because the superficial location of the tumor raises the risk of skin damage (1). In addition, even with proton beam irradiation, it remains unclear where we should irradiate to prevent local recurrence from the edge of the radiation field. Also, in this respect, BNCT is reasonable because we can determine the radiation field by BPA-PET, as described.

There is no report to date, to our knowledge, concerning the application of BNCT to MMs, except for our own first successful case report regarding Patient 1 (23) (see Addendum). As stated here, to our knowledge, there has been only one report in which BPA-PET analysis was applied to MMs (9). The above report and personal communication from Leena Kankaanranta (October 2005) concerning how the T/N ratio of BPA in MMs is 2.5 to 3.5. As stated in the Results section, in our series of BNCT for recurrent malignant gliomas, the T/N ratio determined by BPA-PET study was almost the same as that for the present cases of recurrent MMs. Even in recurrent gliomas, all cases showed radiographic improvement after BNCT (10, 14); therefore, MM might also be a good candidate from this perspective.

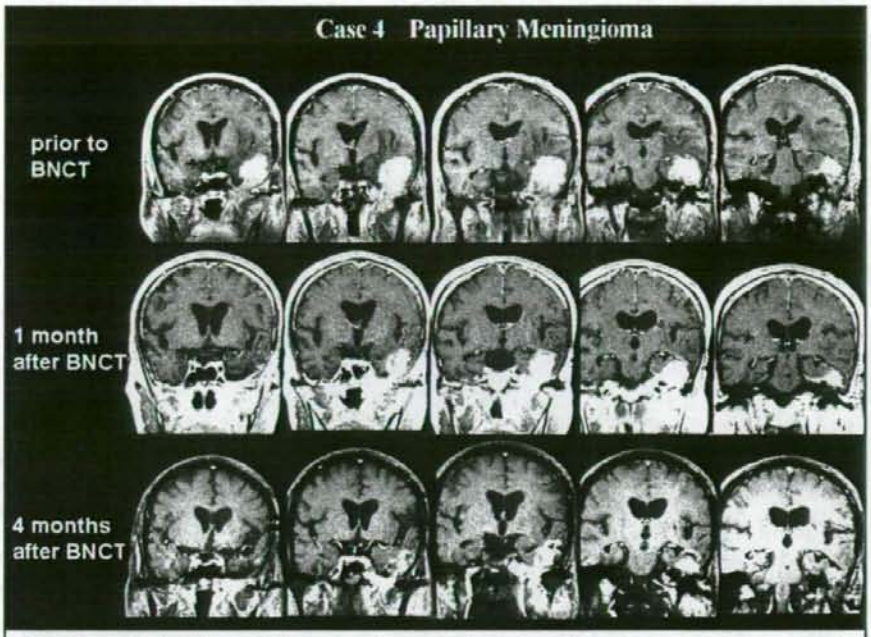

FIGURE 4. *Gd-enhanced coronal MRI scans of Patient 4, who had a papillary meningioma. The homogeneously enhanced tumor shrank gradually in the follow-up images with a decrease in perifocal edema.*

Effects, Limitations, and Side Effects of BNCT for MMs

The short follow-up periods for these patients makes it difficult to assess the effect of BNCT on the survival of patients with MMs. Nonetheless, all of the cases in this series showed clear radiographic improvements, as stated in the Results section (*Table* 2). According to tumor shrinkage, all patients except Patients 4 and 6 showed neurological improvement. In Patients 1 and 3, motor weakness improved immediately after BNCT (23); in Patient 5, both the severe facial pain and the neck pain, which had greatly restricted the activities of daily living score of the patient, were improved by BNCT. All of the changes of Karnofsky Performance Status are depicted in *Table* 3. In Patient 4, no change of Karnofsky Performance Status was observed during the follow-up period, although drastic shrinkage of the mass was observed on MRI scans. In this patient, the activities of daily living score was restricted not by the tumor, but by brainstem infarction. In Patient 6, only limited effectiveness of BNCT was obtained on MRI scanning, with severe brain edema being observed after treatment. This unfavorable response might have been because of the low T/N ratio on BPA-PET and the huge neutron radiation field, which may have caused an excessive absorption of radiation by the healthy brain tissue. In this case, the maximal brain dose was a total of 23.8 Gy-Eq (*Table* 2). On the basis of the present results, it seems that BNCT should be strictly applied to such cases. In Patient 3, the main tumor disappeared in response to BNCT, whereas the other concomitant lesion increased in size, even after BNCT. This was the only case in which tumor recurrence was observed during the observation period. In this case, we could not apply BPA-PET study because of trouble with the machine, as stated. ^{11}C-methioinine did not accumulate at all in this concomitant lesion

TABLE 3. Side effects caused by boron neutron capture therapy with previous radiation treatments[a]

Patient no.	Previous radiation	Side effects	KPS (%)		
			Pre-BNCT	Best	Present
1	SRS 5 times (18, 19, 16, 16, 16 Gy)	RN (9 mo after BNCT)	60	90	60
2	XRT 60 Gy, SRS 18 Gy (whole brain 40 Gy, local 20 Gy)	Brain edema (9 mo after BNCT)	30	40	30
3	SRS 20 Gy	RN (7 mo after BNCT)	60	70	60
4	XRT 54 Gy	—	60	60	60
5	SRS 2 times (12, 12 Gy)	—	60	80	80
6	SRS 2 times (9, 9 Gy)	Brain edema (7 wk after BNCT)	60	60	40

[a] KPS, Karnofsky Performance Status; BNCT, boron neutron capture therapy; present, time of manuscript submission; SRS, stereotactic radiosurgery (doses are marginal doses); RN, radiation necrosis (gadolinium-enhancement with perifocal edema, confirmed with positron emission tomography or surgical specimen); XRT, external radiotherapy.

FIGURE 5. *Gd-enhanced sagittal and coronal MRI scans of Patient 5, who had a sarcoma derived from a meningioma. The three left columns reveal the tumor in the paranasal sinuses and cranial base, and the right column shows cervical lymph node metastasis (*black arrows*). In the sagittal images, tumor shrinkage can be observed; in the coronal images, lymph node metastasis has disappeared completely.*

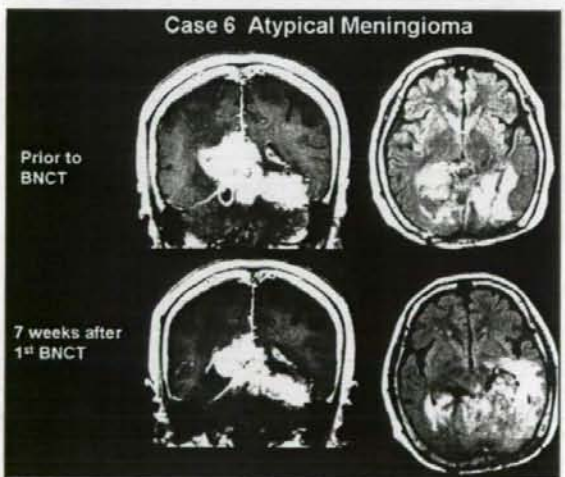

FIGURE 6. *Gd-enhanced (*left*) and fluid-attenuated inversion recovery (*right*) MRI scans of Patient 6. The images in the* top row *were obtained before BNCT. The images in the* bottom row *were obtained 7 weeks after the first BNCT. The enhanced tumor showed a decrease in volume, whereas peritumoral edema increased during this period.*

at the PET just before BNCT, and follow-up repetitive ^{18}F-BPA-PETs revealed an increasing accumulation of the tracer after BNCT. It is speculated that the failure of BNCT to shrink this lesion occurred because of low BPA uptake during BNCT, whereas the main tumor in which BPA accumulated sufficiently disappeared in response to BNCT. As stated in time to progression in *Table 2*, only this case showed tumor recurrence during the observation period, although this period was very limited (see Addendum). All cases reported in this study were referred to our clinic for the treatment of uncontrollable tumor growth. Even with repetitive surgeries or radiotherapy, the tumor recurred within a short interval. In this respect, BNCT may be superior to other treatment modalities.

As stated, BNCT might serve as a potent radiation treatment for MMs; however, all patients introduced to our clinic had been previously treated with radiotherapy. Even by BNCT, healthy neural tissues will inevitably absorb some of the dose. Therefore, there is always some risk of radiation necrosis. In our series, Patients 1, 3, and 6 underwent steroid administration for a long period. The reworsening of Karnofsky Performance Status in Patients 1, 2, 3, and 6 was obviously caused by this radiation side effect. We should keep the possibility of radiation injury in mind, and care should be taken to prevent it. Anticoagulant therapy or vitamin E administration may be effective for the inhibition of radiation necrosis.

Finally, meningiomas tend to have a large blood supply fed by external and, sometimes, internal carotid arteries. Therefore, the maintenance of high concentrations of BSH in feeding vessels might be critical to the successful treatment of MMs, as in Patients 5 and 6. A longer observation period and collection of data from many patients will give us correct indications regarding the use of BNCT for MMs.

REFERENCES

1. Baumert BG, Lomax AJ, Miltchev V, Davis JB: A comparison of dose distributions of proton and photon beams in stereotactic conformal radiotherapy of brain lesions. **Int J Radiat Oncol Biol Phys** 40:1439–1449, 2001.
2. Chadha M, Capala J, Coderre JA, Elowitz EH, Wielopolski L, Chanana AD: Correlation of clinical outcome to the estimated radiation dose from BNCT, in Larsson B, Crawford J, Weinreich R (eds): *Advances in Neutron Capture*

Therapy: Chemistry and Biology. Amsterdam, Elsevier Science Publishers B.V., 1997, vol 2, pp 575–579.
3. Dziuk TW, Woo S, Butler EB, Thornby J, Grossman R, Dennis WS, Lu H, Carpenter LS, Chiu JK: Malignant meningioma: An indication for initial aggressive surgery and adjuvant radiotherapy. **J Neurooncol** 37:177–188, 1998.
4. Fukushima T, Tsugu H, Tomonaga M, Shirakusa T: Papillary meningioma with pulmonary metastasis. Case report. **J Neurosurg** 70:478–482, 1989.
5. Hug EB, Devries A, Thornton AF, Munzenrider JE, Pardo FS, Hedley-Whyte ET, Bussiere MR, Ojemann R: Management of atypical and malignant meningiomas: Role of high-dose, 3D-conformal radiation therapy. **J Neurooncol** 48:151–160, 2000.
6. Imahori Y, Ueda S, Ohmori Y, Sakae K, Kusuki T, Kobayashi T, Takagaki M, Ono K, Ido T, Fujii R: Positron emission tomography-based boron neutron capture therapy using boronophenylalanine for high-grade gliomas: Part I. **Clin Cancer Res** 4:1825–1832, 1998.
7. Imahori Y, Ueda S, Ohmori Y, Sakae K, Kusuki T, Kobayashi T, Takagaki M, Ono K, Ido T, Fujii R: Positron emission tomography-based boron neutron capture therapy using boronophenylalanine for high-grade gliomas: Part II. **Clin Cancer Res** 4:1833–1841, 1998.
8. Jääskeläinen J, Haltia M, Servo A: Atypical and anaplastic meningiomas: Radiology, surgery, radiotherapy, and outcome. **Surg Neurol** 25:233–242, 1986.
9. Joensuu H, Kankaanranta L, Seppala T, Auterinen I, Kallio M, Kulvik M, Laakso J, Vahatalp J, Kortesniemi M, Kotiluoto P, Seren T, Karrila J, Brander A, Jarviluoma E, Ryynannen P, Paetau A, Ruokonen I, Minn H, Tenhunen M, Jääskeläinen J, Farkkila M, Savolainen S: Boron neutron capture therapy of brain tumors: Clinical trials at the finnish facility using boronophenylalanine. **J Neurooncol** 62:123–134, 2003.
10. Kawabata S, Miyatake S, Kajimoto Y, Kuroda Y, Kuroiwa T, Imahori Y, Kirihata M, Sakurai Y, Kobayashi T, Ono K: The early successful treatment of glioblastoma patients with modified boron neutron capture therapy. Report of two cases. **J Neurooncol** 65:159–165, 2003.
11. Kinashi Y, Masunaga SI, Suzuki M, Ono K, Ohnishi T: Hyperthermia enhanced thermal-neutron-induced cell death of human glioblastoma cell lines at low concentration of ^{10}B. **Int J Rad Oncol Biol Phys** 40:1185–1192, 1998.
12. Louis DN, Scheithauer BW, Budka H, Von Deimling A, Kepes JJ: Meningiomas, in Kleihues P, Cavenee WK (eds): *Pathology and Genetics of Tumours of the Nervous System*. Lyon, IARC Press, 2000, pp 176–184.
13. Mahmood A, Caccamo DV, Tomecek FJ, Malik GM: Atypical and malignant meningiomas: A clinicopathological review. **Neurosurgery** 33:955–963, 1993.
14. Miyatake S, Kawabata S, Kajimoto Y, Aoki A, Yokoyama K, Yamada M, Kuroiwa T, Tsuji M, Imahori Y, Kirihata M, Sakurai Y, Masunaga S, Nagata K, Maruhashi A, Ono K: Modified boron neutron capture therapy for malignant gliomas performed using epithermal neutron and two boron compounds with different accumulation mechanisms: An efficacy study based on findings on neuroimages. **J Neurosurg** 103:1000–1009, 2005.
15. Morris GM, Coderre JA, Hopewell JW: Evaluation of CNS toxicity to BNCT type irradiation using a rat spinal cord model, in Larsson B, Crawford J, Weinreich R (eds): *Advances in Neutron Capture Therapy: Chemistry and Biology*. Amsterdam, Elsevier Science Publishers B.V., 1997, vol 2, pp 665–669.
16. Ojemann SG, Sneed PK, Larson DA, Gutin PH, Berger MS, Verhey L, Smith V, Petti P, Wara W, Park E, McDermott MW: Radiosurgery for malignant meningioma: Results in 22 patients. **J Neurosurg** 93[Suppl 3]: 62–67, 2000.
17. Ono K, Masunaga SI, Kinashi Y, Takagaki M, Akaboshi M, Kobayashi T, Akuta K: Radiobiological evidence suggesting heterogenous microdistribution of boron compounds in tumors: Its relation to quiescent cell population and tumor cure in neutron capture therapy. **Int J Radiat Oncol Biol Phys** 34:1081–1086, 1996.
18. Pack GT, Ariel IM (eds): *Treatment of Cancer and Allied Diseases*. New York, Harper & Brothers, 1959, p 59.
19. Palma L, Celli P, Franco C, Cervoni L, Cantore G: Long-term prognosis for atypical and malignant meningiomas: A study of 71 surgical cases. **J Neurosurg** 86:793–800, 1997.
20. Russel DS, Rubinstein LJ: *Pathology of Tumours of the Nervous System: Primary Meningeal and Cerebral Sarcomas*. London, Butler & Tanner Ltd., 1989, ed 5, pp 507–517.
21. Salazar OM: Ensuring local control in meningiomas. **Int J Radiat Oncol Biol Phys** 15:501–504, 1988.
22. Simpson D: The recurrence of intracranial meningiomas after surgical treatment. **J Neurol Neurosurg Psychiatry** 20:22–39, 1957.
23. Tamura Y, Miyatake SI, Nonoguchi N, Miyata S, Yokoyama K, Doi A, Kuroiwa T, Asada M, Tanabe H, Ono K: Boron neutron capture therapy for recurrent malignant meningioma: Report of first trial. **J Neurosurg** 105:898–903, 2006.
24. Tayler HJ, Goldhaber M: Detection of nuclear disintegration in a photographic emulsion. **Nature** 135:341, 1935.

Acknowledgments

This work was partly supported by a Grant-in-Aid for Scientific Research, Grant B-16390422, from the Japanese Ministry of Education, Science, and Culture; by a grant from the Regional Science Promotion Program of the Japan Science and Technology Corporation; and by a grant from the "Second-term Comprehensive 10-Year Strategy for Cancer Control" of the Ministry of Health, Labor, and Welfare of Japan to Shin-Ichi Miyatake. This work was also supported in part by the Takeda Science Foundation for OMC. The research was also supported in part by a Grant-in-Aid for Cancer Research from the Ministry of Education, Culture, Sports, Science, and Technology of Japan, Grant 12217065, to Koji Ono, M.D, Ph.D.

ADDENDUM

These events occurred after the submission of this manuscript:

1) In Patient 1, no recurrence has been recognized in the BNCT radiation field. However, a new lesion at the left frontal base including an intraorbital extension was identified on the follow-up MRI scan taken 14 months after BNCT.
2) In Patient 4, no recurrence was found on the MRI scan taken 8 months after BNCT. Nine months after BNCT, however, results of MRI scanning revealed regrowth of the tumor at the left cavernous sinus. This recurrence point was deepest in the radiation field.
3) Patient 6 died 8 months after BNCT from sepsis and disseminated intravascular coagulation, probably caused by the side effects of the steroids.
4) At the 12th International Congress on Neutron Capture Therapy in Kagawa, Japan, October 2006, Dr. Britta H. Stenstam (Studivik Medical AB, Nykoping, Sweden) reported that the Swedish BNCT group also treated some cases of MM by BNCT.

COMMENTS

This is an interesting study showing definite activity of boron neutron capture therapy (BNCT) in patients with difficult, advanced Grade III meningiomas, a mostly hopeless group. BNCT is not being done much in this country, and I don't think that finding this activity in malignant meningiomas will make us reconsider this for the following reasons: 1) anaplastic meningiomas are rare; 2) they are frequently diffuse, multifocal, invasive, and/or metastatic, making radiation targeting of all kinds problematic; and 3) BNCT is a technology intensive and labor intensive treatment with societal safety implications and, until now, has been almost entirely based at nuclear reactors like the Kyoto University Research Reactor Institute where this study and a recent study of gliomas by the same group (1) were conducted.

Philip H. Gutin
New York, New York

---

1. Miyatake SI, Kawabata S, Kajimoto Y, Aoki A, Yokoyama K, Yamada M, Kuroiwa T, Tsuji M, Imahori Y, Kirihata M, Sakurai Y, Masunaga SI, Nagata K,

Maruhashi A, Ono K: Modified boron neutron capture therapy for malignant gliomas performed using epithermal neutron and two boron compounds with different accumulation mechanisms: An efficacy study based on findings on neuroimages. **J Neurosurg** 103:1000–1009, 2005.

The authors have demonstrated an interesting application of BNCT for high-grade meningiomas. These tumors typically fail surgery, conventional radiation therapy, and radiosurgery, and there are no good chemotherapy options. Although BNCT is available in few locations, the results of this initial study of a small cohort of patients provides interesting results. Further application of BNCT in this population is merited, and one hopes the authors will expand this series to a larger number of patients and report longer-term follow-up data. This is the first promising treatment option for high-grade meningiomas in a long time.

Joseph M. Piepmeier
New Haven, Connecticut

Magic bullets are hard to find for malignant meningioma patients. Once a tumor is defined as World Health Organization Grade 3 or has sarcomatous elements, the tumor defies any of a number of surgical, radiation therapeutic, radiosurgical, and chemotherapeutic options. And once a patient has reached the stage of defined failure of these more conventional options, additional therapies can be expected to provide little measurable benefit in either longevity or quality of life. Life expectancy after diagnosis averages approximately 7 years, even with repeated application of therapeutic options. The report from the experience in Japan reemphasizes the problems, yet attempts to define a clinical indication for what must be an amazingly resource intensive program. The periodic resurfacing of boron projects testifies to the amazing resilience of a form of radiation that has required extensive resource investment but has resulted in amazingly little clinical benefit to date. I am not sure that this late term investment in BNCT provides any evidence of safety or efficacy. The main consistency in this report lies in the fact that the six patients had aggressive meningiomas and received neutrons in some form in one or more sessions. Because all the patients had already failed surgery and radiation therapy or multiple sessions of radiosurgery, it is not unexpected that three out of six experienced either radiation necrosis or worsened edema, although contrast enhancement on follow-up magnetic resonance imaging scans is not necessarily indicative of adverse radiation effects. Certainly, it would seem premature to state that BNCT as used in this paradigm, and potentially any other, has any benefit for central nervous system tumors. The value of high linear energy transfer radiation modalities has been difficult to match with their resource costs. After each of its rebirths, the concept of superior response of BNCT and its enhanced "gray equivalents," as the authors note, remain "theoretical."

L. Dade Lunsford
Pittsburgh, Pennsylvania

Although BNCT has fallen out of favor and clearly has very limited usefulness, the authors of this study present a number of cases in which it was logical to attempt this type of therapy, particularly as nothing else seems to be effective for atypical meningiomas that act in a malignant fashion. The cases presented do show some beneficial effect of the BNCT. It will be critical to evaluate whether or not the patients developed any evidence of cognitive dysfunction or neurological deficit that might be attributable to the effects of radiation over time. This is drastic therapy for a difficult type of tumor. One can still hope that a newer selectively delivered boron compounds may be developed that will enhance the effectiveness of this intriguing mode of therapy.

Edward R. Laws, Jr.
Stanford, California

IN-TRAINING LIAISONS

The Congress of Neurological Surgeons exists for the purpose of promoting public welfare through the advancement of neurosurgery by a commitment to excellence in education and by a dedication to research and scientific knowledge.

—Mission Statement
Congress of Neurological Surgeons

Inherent in this commitment is a critical charge to serve the needs of the in-training individuals. Considering the importance of this vital group within the neurosurgical community, the Journal has established a position within its board structure termed **In-training Liaison.** The individuals holding this position will act as spokespersons especially addressing the needs and concerns of individuals in in-training positions globally, as they relate to journal content and perspective.

The current individuals holding this position are:

Rahul Jandial, M.D. and Matthew J. McGirt, M.D.

Issues attendant to in-training matters should be conveyed to Dr. Rahul Jandial at the Division of Neurological Surgery, University of California, San Diego Medical Center, 200 West Arbor Drive, Mail Code 8893, San Diego, California 92103, or Dr. Matthew J. McGirt at the Department of Neurosurgery, The Johns Hopkins Hospital, 600 North Wolfe Street, Meyer 8-161, Baltimore, Maryland 21287.

email: rjandial@ucsd.edu or mmcgirt1@jhmi.edu

J Neurosurg 106:507–510, 2007

Endoscopic identification and biopsy sampling of an intraventricular malignant glioma using a 5–aminolevulinic acid–induced protoporphyrin IX fluorescence imaging system

Technical note

YOJI TAMURA, M.D.,[1] TOSHIHIKO KUROIWA, M.D.,[1] YOSHINAGA KAJIMOTO, M.D.,[1] YOSHIHITO MIKI, M.D.,[1] SHIN-ICHI MIYATAKE, M.D.,[1] AND MASAO TSUJI, M.D.[2]

[1]Department of Neurosurgery, Osaka Medical College, Takatsuki; and [2]Department of Neurosurgery, Nishinomiya Kyoritsu Neurosurgical Hospital, Nishinomiya, Japan

✓Several neurosurgical studies have provided descriptions of the utility of fluorescence-guided tumor resection using a microscope. However, fluorescence-guided endoscopic detection of a deep-seated brain tumor has not yet been reported. The authors report their experience with an endoscopic biopsy procedure for a malignant glioma within the third ventricle using a 5–aminolevulinic acid (5-ALA)–induced protoporphyrin IX fluorescence imaging system. A 5-ALA–induced fluorescence image of an intraventricular tumor is barely visible with the typical fluorescence endoscopic system used in other clinical fields because the intensity of excitation light at wavelengths of 390 to 405 nm through a cutoff filter is too weak to delineate a brain tumor.

The technique described in this study made use of a laser illumination system with a high-powered output that delivered a violet-blue light at wavelengths of 405 nm. In addition, a common ultraviolet cutoff filter was fitted between the endoscope and the high-sensitivity camera to block the backscattered excitation light. A 5-ALA–induced fluorescence endoscopy performed using this system allowed the intraventricular tumor to be clearly visualized as a red fluorescent lesion. Several biopsy specimens obtained from the fluorescent lesion provided a definitive histological diagnosis. The results indicate that this endoscopic system is useful in detecting an intraventricular fluorescent tumor.

KEY WORDS • **intraventricular malignant glioma** • **5–aminolevulinic acid** • **biopsy** • **photodynamic diagnosis** • **fluorescence-guided resection**

In recent years, photodynamic diagnosis and therapy for high-grade malignant gliomas have received increasing attention.[5,6,11–15] Fluorescent dyes that include fluorescein sodium,[6,13] 5-ALA,[11,15] and porfimer sodium[12] are used for photodynamic diagnosis and therapy. A surgical microscope with a fluorescence system can facilitate the resection of malignant gliomas because fluorescent images enable the surgeon to discriminate between the tumor tissue and the surrounding brain tissues.[6,15] In clinical fields other than neurosurgery, several studies have been conducted to investigate the fluorescence endoscopic detection of premalignant and malignant lesions.[1,4,7,10,16] However, there has been no report of a photodynamic diagnosis of a deep-seated brain tumor using fluorescence endoscopy, primarily because the fluorescence intensity under ordinary excitation light is too weak to allow observation of the central nervous system. Therefore, we developed a 5-ALA–induced fluorescence endoscopic system equipped with a high-powered laser light source. In this report we describe the clinical usefulness of a fluorescence endoscopic detection and biopsy procedure for an intraventricular malignant glioma.

Abbreviations used in this paper: BBB = blood–brain barrier; CSF = cerebrospinal fluid; 5-ALA = 5–aminolevulinic acid.

Operative Technique

A flexible fiberscope with an external diameter of 4.2 mm (N-4L, Machida) was used for the procedure. The fiberscope was connected to either a light source delivering common white light (Olympus) or to a laser illumination system delivering ultraviolet laser light (BP-300, Ball Semiconductor, Inc.). This laser system was equipped with a bundle of 16 optical fibers emitting a 405 nm wavelength laser and a 300-mW high-powered output. An ultraviolet cutoff filter (Wratten No. 2E, Kodak) was inserted between the ocular lens of the fiberscope and the high-sensitivity 2D charge-coupled device camera (Hamamatsu Photo) to cut off reflective light, including excitation light. This filter does not influence the normal color tone of the image, so it

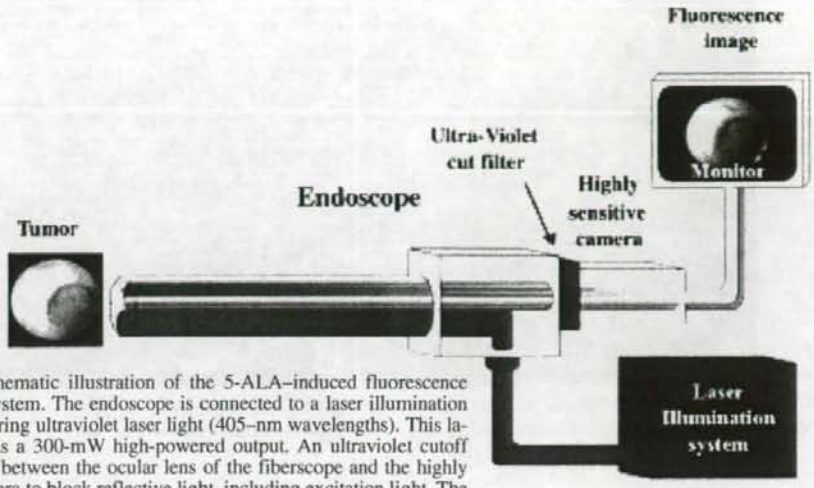

FIG. 1. Schematic illustration of the 5-ALA–induced fluorescence endoscopic system. The endoscope is connected to a laser illumination system delivering ultraviolet laser light (405–nm wavelengths). This laser system has a 300-mW high-powered output. An ultraviolet cutoff filter is fitted between the ocular lens of the fiberscope and the highly sensitive camera to block reflective light, including excitation light. The camera detects fluorescent light and displays images on a monitor.

does not need to be changed between the common white light and laser light modes. The camera was used to capture fluorescence images by gathering background autofluorescence in normal brain tissue and 630 nm wavelength red fluorescence in the malignant tumor; the images were then depicted on a monitor (Fig. 1).

Illustrative Case

History and Examination. This 56-year-old woman presented with a 1-month history of progressive headaches and diplopia. Magnetic resonance images demonstrated hydrocephalus due to a nonenhancing midbrain mass lesion. The patient underwent an endoscopic tumor biopsy procedure and third ventriculostomy at a nearby hospital. Her histological examination revealed a possible low-grade glioma because the removed specimens were small. She did not receive adjuvant therapy for this tumor. However, 6 months later she again presented with diplopia. Additional magnetic resonance images showed a ring-enhancing lesion in the same midbrain area (Fig. 2). The patient was referred to our hospital for a definitive diagnosis and further treatment.

Fluorescence Endoscopic Biopsy Procedure. We obtained approval to perform the fluorescence endoscopic biopsy procedure from the Ethical Committees of Osaka Medical College. Four hours before surgery, the patient received 20 mg/kg of 5-ALA (Medac GmbH) dissolved in water and administered orally. After anesthesia was induced, the right lateral ventricle was cannulated with a No. 16 peelaway catheter. The fiberscope was inserted into the third ventricle through the foramen of Monro, and a good CSF flow through the previous stoma was identified by floor pulsation. The endoscope was passed farther into the posterior third ventricle and a protruding lesion was visualized at the entrance of the aqueduct. Under white light, this lesion was similar in color to the surrounding brain tissue (Fig. 3A). When the light source of the endoscope was changed to the laser light, the lesion emitted a red fluorescence (Fig. 3B). Using small forceps, several biopsy samples were taken from this red fluorescent lesion.

Postoperative Course. The histological diagnosis of the biopsy specimens was consistent with anaplastic astrocytoma (Fig. 4). The patient received local radiotherapy totaling 60 Gy and chemotherapy with nitrosourea. Her visual symptoms responded well to these therapies, and she was able to walk without aid.

Discussion

We previously used fluorescein sodium as a fluorescent dye in the microscopic photodynamic diagnosis of malignant gliomas.[5,6] Fluorescein sodium passes into the brain tissue and brain tumor through the vessels, including the capillaries, where the BBB is absent or disrupted. Following intravenous administration of fluorescein sodium, all of the tissues without a BBB emit green fluorescence. We have

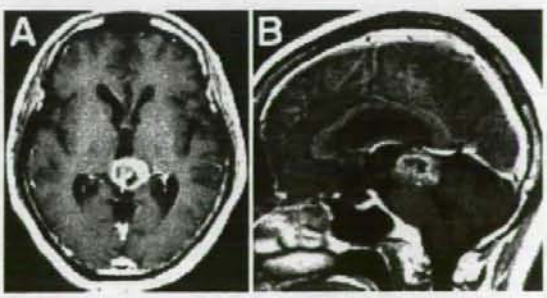

FIG. 2. Axial (A) and sagittal (B) T_1-weighted magnetic resonance images with contrast showing a heterogeneous enhanced mass in the posterior portion of the third ventricle.

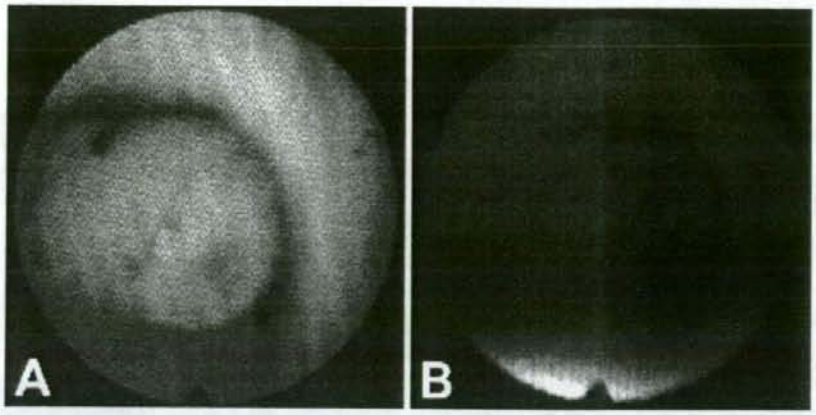

FIG. 3. Endoscopic photographs of the entrance of the aqueduct *(star)*. Compared with a typical endoscopic image system (A), the 5-ALA–induced fluorescence endoscopic system shows a red fluorescent mass (B).

often been unable to discriminate between tumor tissues and peritumoral vasogenic edema using the fluorescence microscopic system. Fluorescein sodium was not suitable for intraventricular tumor detection by the endoscope because it rapidly diffuses into the CSF.

In contrast, 5-ALA is absorbed into both normal and tumor tissues, whereas the metabolite protoporphyrin IX accumulates selectively in the tumor tissue. This difference is probably due to altered activity levels of the enzymes of the heme biosynthetic pathway within the transformed cells.[3,16] Only protoporphyrin IX within the tumor emits red fluorescence under violet-blue light; therefore, 5-ALA is a promising fluorescent dye to use in inspection of the CSF space.

In neurosurgery, 5-ALA–induced fluorescence has been used only in conjunction with a surgical microscope. Stummer and colleagues[14] reported the usefulness of fluorescence-guided resection with 5-ALA–induced porphyrins for glioblastomas. However, there has not been a report on efforts to detect a brain tumor under an endoscopic fluorescence image using 5-ALA. In the oropharyngolarynx, bladder, uterus, gastrointestinal system, and other areas within the body that do not have a barrier such as the BBB, 5-ALA can easily move from the blood vessels to the neoplasm. Therefore, protoporphyrin IX emits relatively stable fluorescence, and it is possible to detect the fluorescent lesion using fluorescence endoscopy.[1,4,7,10,16]

In the conventional fluorescence endoscopic system, a 300-mW short-arc xenon light source is used. This instrument is equipped with a dielectric short-pass filter (375–440 nm wavelengths), which exchanges a white light for a violet-blue light so that the intensity of the excitation light is decreased. For this reason, it was difficult to detect a red fluorescent intraventricular tumor by the ordinary system (unpublished data). In the present endoscopic system, we provided a high-powered laser illumination system as a light source. This 405 nm–wavelength laser light delivers an excitation light that ensures an adequate 5-ALA–induced fluorescence intensity in the central nervous system. Because an ultraviolet cutoff filter that blocked the backscattered excitation laser light was inserted between the endoscope and the camera, the intraventricular structure and the tumor were visible under both the white light and the laser light without having to change the filter. This system is simple and economical. Therefore, its clinical application is promising for fluorescence endoscopic detection of malignant brain tumors.

Due to the limited penetration depth of protoporphyrin IX,[8] it is, however, difficult to use a fluorescence image to detect a tumor that is covered with brain tissue, except for the thin ependymal layer. If technical advances in fluorescence images are able to solve this problem, it would be possible to locate not only intraventricular but also intraparenchymal tumors. Moreover, if the ongoing photodynamic therapy research on malignant tumors[2,9,11,12] becomes established in the foreseeable future, we can speculate that the fluorescence endoscopic system has a good chance of

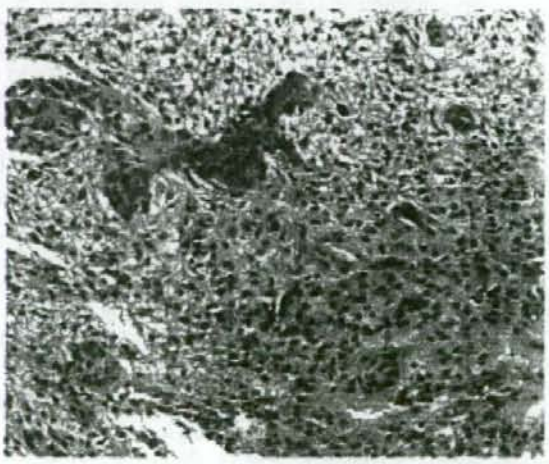

FIG. 4. Photomicrograph of tumor tissue obtained from the red fluorescent area in Fig. 3 showing high cellularity, pleomorphism, and endothelial proliferation. The tumor was later diagnosed as an anaplastic astrocytoma. H & E, original magnification × 100.

becoming the preferred treatment for deep-seated brain tumors.

Conclusions

We developed a simple and economical fluorescence endoscopic system that was very useful for intraoperative detection and diagnosis of malignant gliomas in the third ventricle. We expect that this system will form the basis for fluorescence endoscopic neurosurgery in the future.

References

1. Endlicher E, Knuechel R, Hauser T, Szeimies RM, Scholmerich J, Messmann H: Endoscopic fluorescence detection of low and high grade dysplasia in Barrett's oesophagus using systemic or local 5-aminolaevulinic acid sensitization. **Gut 48:**314–319, 2001
2. Ito S, Rachinger W, Stepp H, Reulen HJ, Stummer W: Oedema formation in experimental photo-irradiation therapy of brain tumors using 5-aLA. **Acta Neurochir (Wien) 147:**57–65, 2005
3. Kennedy JC, Pottier RH: Endogenous protoporphyrin IX, a clinically useful photosensitizer for photodynamic therapy. **J Photochem Photobiol B 14:**275–292, 1992
4. Kriegmair M, Zaak D, Rothenberger KH, Rassweiler J, Jocham D, Eisenberger F, et al: Transurethral resection for bladder cancer using 5-aminolevulinic acid induced fluorescence endoscopy versus white light endoscopy. **J Urol 168:**475–478, 2002
5. Kuroiwa T, Kajimoto Y, Ohta T: Comparison between operative findings on malignant glioma by a fluorescein surgical microscopy and histological findings. **Neurol Res 21:**130–134, 1999
6. Kuroiwa T, Kajimoto Y, Ohta T: Development of a fluorescein operative microscope for use during malignant glioma surgery: a technical note and preliminary report. **Surg Neurol 50:**41–49, 1998
7. Leunig A, Betz CS, Mehlmann M, Stepp H, Arbogast S, Grevers G, et al: Detection of squamous cell carcinoma of the oral cavity by imaging 5-aminolevulinic acid-induced protoporphyrin IX fluorescence. **Laryngoscope 110:**78–83, 2000
8. Leunig A, Mehlmann M, Betz C, Stepp H, Arbogast S, Grevers G, et al: Fluorescence staining of oral cancer using a topical application of 5-aminolevulinic acid: fluorescence microscopic studies. **J Photochem Photobiol B 60:**44–49, 2001
9. Madsen SJ, Angell-Petersen E, Spetalen S, Carper SW, Ziegler SA, Hirschberg H: Photodynamic therapy of newly implanted glioma cells in the rat brain. **Lasers Surg Med 38:**540–548, 2006
10. Messmann H, Endlicher E, Freunek G, Rummele P, Scholmerich J, Knuchel R: Fluorescence endoscopy for the detection of low and high grade dysplasia in ulcerative colitis using systemic or local 5-aminolaevulinic acid sensitization. **Gut 52:**1003–1007, 2003
11. Olzowy B, Hundt CS, Stocker S, Bise K, Reulen HJ, Stummer W: Photoirradiation therapy of experimental malignant glioma with 5-aminolevulinic acid. **J Neurosurg 97:**970–976, 2002
12. Popovic EA, Kaye AH, Hill JS: Photodynamic therapy of brain tumors. **J Clin Laser Med Surg 14:**251–261, 1996
13. Shinoda J, Yano H, Yoshimura S, Okumura A, Kaku Y, Iwama T, et al: Fluorescence-guided resection of glioblastoma multiforme by using high-dose fluorescein sodium. Technical note. **J Neurosurg 99:**597–603, 2003
14. Stummer W, Novotny A, Stepp H, Goetz C, Bise K, Reulen HJ: Fluorescence-guided resection of glioblastoma multiforme by using 5-aminolevulinic acid-induced porphyrins: a prospective study in 52 consecutive patients. **J Neurosurg 93:**1003–1013 2000
15. Stummer W, Stocker S, Wagner S, Stepp H, Fritsch C, Goetz C: Intraoperative detection of malignant gliomas by 5-aminolevulinic acid-induced porphyrin fluorescence. **Neurosurgery 42:** 518–526, 1998
16. Zaak D, Hungerhuber E, Schneede P, Stepp H, Frimberger D, Corvin S, et al: Role of 5-aminolevulinic acid in the detection of urothelial premalignant lesions. **Cancer 95:**1234–1238, 2002

Manuscript submitted March 22, 2006.
Accepted July 13, 2006.

Address reprint requests to: Yoji Tamura, M.D., Department of Neurosurgery, Osaka Medical College, 2–7, Daigaku-machi, Takatsuki City, Osaka 569–8686, Japan. email: neu034@poh.osaka-med.ac.jp.

J Neurooncol (2007) 83:223–231
DOI 10.1007/s11060-006-9325-8

LABORATORY INVESTIGATION

Massive apoptotic cell death of human glioma cells via a mitochondrial pathway following 5-aminolevulinic acid-mediated photodynamic therapy

Hiroto Inoue · Yoshinaga Kajimoto · Masa-Aki Shibata · Norio Miyoshi · Naoko Ogawa · Shin-Ichi Miyatake · Yoshinori Otsuki · Toshihiko Kuroiwa

Received: 11 November 2005 / Accepted: 29 December 2006 / Published online: 24 January 2007

Abstract The basic mechanism of cell death induced by 5-aminolevulinic acid (5-ALA)-mediated photodynamic therapy (PDT) (ALA-PDT) in glioma cells has not been fully elucidated. In this study, the details of the cell death mechanism induced by ALA-PDT were investigated in three human glioma cell lines (U251MG, U87MG, and U118MG) *in vitro*. To evaluate the manner of accumulation of protoporphyrin IX (PpIX), intracellular PpIX contents were measured by flow cytometry after incubation with 5-ALA. To analyze the mechanism of cell death, U251MG cells were assayed by the terminal deoxynucleotidyl transferase-mediated dUTP-FITC nick end-labeling (TUNEL) method, and the caspase activity was measured after ALA-PDT. Furthermore, the mitochondrial membrane potential (MMP) and the release of mitochondrial cytochrome *c* were determined. PpIX fluorescence reached a plateau 4 h after exposure to 5-ALA. The proportion of dead cells increased with increases in the dosage of light. These cells were confirmed by TUNEL staining to be apoptotic. Increases in the activity of both caspase-3 and -9, a decrease in MMP, and a marked increase in cytochrome *c* in the cytosolic fraction were found after cells were subjected to PDT. These results indicate that a dysfunction of MMP is followed by mitochondrial cytochrome *c* release, which triggers apoptosis through a mitochondrial pathway. ALA-PDT induces massive apoptosis due to the direct activation of a mitochondrial pathway, which is resistant to many anti-apoptotic processes, in human glioma cells. This finding implies that ALA-PDT is a promising therapy for the treatment of apoptosis-reluctant tumors such as malignant gliomas.

Keywords Apoptosis · Caspase · Cytochrome *c* · 5-Aminolevulinic acid · Glioma · Photodynamic therapy

Abbreviations

5-ALA	5-aminolevulinic acid
MMP	mitochondrial membrane potential
PDT	photodynamic therapy
PpIX	protoporphyrin IX
TUNEL	terminal deoxynucleotidyl transferase-mediated dUTP-FITC nick end-labeling

H. Inoue · Y. Kajimoto (✉) · M.-A. Shibata · N. Miyoshi · N. Ogawa · S.-I. Miyatake · Y. Otsuki · T. Kuroiwa
Department of Neurosurgery, Osaka Medical College, 2-7 Daigaku-machi, Takatsuki, Osaka, Japan
e-mail: neu039@poh.osaka-med.ac.jp

H. Inoue · Y. Kajimoto · M.-A. Shibata · N. Miyoshi · N. Ogawa · S.-I. Miyatake · Y. Otsuki · T. Kuroiwa
Department of Anatomy and Biology, Osaka Medical College, Takatsuki, Osaka, Japan

H. Inoue · Y. Kajimoto · M.-A. Shibata · N. Miyoshi · N. Ogawa · S.-I. Miyatake · Y. Otsuki · T. Kuroiwa
Department of Pathology, University of Fukui, Fukui, Japan

Introduction

Improvements in progression-free survival and overall survival in patients with malignant gliomas have not been achieved in spite of intensive treatment, including surgical resection, postoperative radiation therapy, and

chemotherapy. The median survival time is currently less than 12 months [36]. As the failure of treatment is usually due to insufficient local control of the site of surgical resection, novel local therapies are still necessary. Photodynamic therapy (PDT) is a promising type of local therapy, and favorable results have been reported in several studies of PDT in glioma patients [17, 18, 21, 27, 34].

Protoporphyrin IX (PpIX), which is synthesized from 5-aminolevulinic acid (5-ALA) in mitochondria, is an intrinsic and safe photosensitizer. PpIX is known to accumulate in several malignant tumors by the administration of 5-ALA, and this phenomenon is widely applicable for photodynamic diagnosis and PDT [8, 9, 31, 32].

PDT is able to induce diverse cellular responses, including apoptosis, in which cells undergo characteristic biochemical and morphological changes [1, 25, 29, 42]. Caspases, a class of cysteine proteases, play a crucial role in the execution of apoptosis [26, 28]. The release of cytochrome *c* from mitochondria is a critical step in many apoptotic pathways [13, 22]. Although 5-ALA-mediated PDT (ALA-PDT) can induce apoptosis, little is known about the signaling cascades involved in this process. In particular, there has not yet been a report accounting for the details of the mechanism of death induced by ALA-PDT in human glioma cells.

In the present study, we investigated the accumulation of 5-ALA-induced PpIX and the death-inducing effect of ALA-PDT on human glioma cell lines. To determine this particular cell death pathway, the terminal deoxynucleotidyl transferase-mediated dUTP-FITC nick end-labeling (TUNEL) method was performed. Furthermore, activities of caspase-3, -8, and -9 were measured in cells that had undergone ALA-PDT. Moreover, to investigate the involvement of a mitochondrial pathway in apoptosis after ALA-PDT, decreases in the mitochondrial membrane potential (MMP) and the release of cytochrome *c* were determined.

Materials and methods

Cell lines and cell culture

The human glioblastoma cell lines (U251MG, U87MG, and U118MG) used in this study were purchased from American Type Culture Collection (Manassas, VA). The cells were cultured in a monolayer in Dulbecco's Modified Eagle's Medium (DMEM; Invitrogen, Tokyo, Japan) buffered with 25 mM bicarbonate and supplemented with 10% heat-inactivated fetal bovine serum (FBS; Invitrogen, Grand Island, NY) in a fully humidified incubator at 37(C with 5% CO_2.

Pp IX accumulation in lined human glioma cells incubated with 5-ALA

Confluent cells were used in the following experiments. 5-ALA was dissolved in bicarbonate-buffered DMEM with 10% FBS to achieve a final concentration of 1 mM, buffered to pH 7.4 with 1 M NaOH, and then the solution was added to the dishes. This concentration of 5-ALA was then used in the following experiments. Incubation continued for 8 h in the dark. The intracellular PpIX contents were measured at 1 h intervals by flow cytometry analysis with EPICS ELITE ESP (Beckman Coulter, Inc., Miami, FL, U.S.A.) using 2×10^4 cells for each determination. Fluorescence from intracellular PpIX was excited by an argon ion laser line at 488 nm, and the fluorescence was detected at 635 nm using a 600 nm longpass filter. The results were based on three independent experiments.

Phototoxicity evaluated by scattergrams using a flow cytometer

For the determination of phototoxicity, U251MG cells treated with 5-ALA for 4 h were exposed to violet-blue light (approximately 405 nm). The fluence rate of the light reaching the cells was approximately 1 mW/cm^2, and the total doses were 0.1, 0.2, 0.5, and 1.0 J/cm^2. The medium was immediately replaced after illumination with DMEM containing 10% FBS. Damage to the cells was detected using a flow cytometer 24 h after photoirradiation. Upon flow cytometric examination, damaged cells, both apoptotic and necrotic cells, could be detected by light scatter changes characterized decreased forward scatter and increased side scatter. In order to clarify the detailed mechanism of phototoxicity, following three independent experiments were performed.

TUNEL staining

U251MG cells treated with 5-ALA for 4 h were irradiated with light doses of 0.1, 0.2, 0.3, and 0.4 J/cm^2. Twenty-four hours after PDT, the cells were assayed by the TUNEL method using the MEBSTAIN apoptosis kit direct (MBL, Inc., Nagoya, Japan) for the flow cytometric analysis, and an apoptosis in situ

detection kit (Wako Pure Chemicals, Osaka, Japan) for the microscopic observation. Untreated cells were used as a control.

Microscopic observation of apoptotic cells using TUNEL staining

The cells were fixed with 4% paraformaldehyde for 30 min at 4°C, washed with phosphate-buffered saline (PBS), and permeabilized with 0.1% Triton X-100 for 2 min on ice. After washing the cells with PBS, they were incubated with terminal deoxynucleotidyl transferase and FITC-dUTP for 10 min at 37°C, rinsed with PBS, and exposed to anti-FITC-peroxidase for 10 min at 37°C. Apoptotic cells were visualized using diaminobentidine/H_2O_2 and 0.5% methyl green staining.

Flow cytometric analysis of apoptotic cells using TUNEL staining

The cells were fixed as described above, washed with bovine serum albumin-phosphate-buffered saline (BSA-PBS), and permeabilized with 70% ethanol for 30 min at –20°C. After washing the cells with BSA-PBS, they were incubated with terminal deoxynucleotidyl transferase and FITC-dUTP for 60 min at 37°C. The cells were then rinsed with BSA-PBS and measured using a flow cytometer.

Caspase activity

The activities of caspase-3, -8, and -9 were measured in U251MG cells 24 h after PDT (0.2 J/cm^2), as described above (n = 5); untreated cells were used as a control (n = 5). A fluorometric protease assay kit (MBL, Inc., Nagoya, Japan) was used for the analysis. In this assay, the cells were lysed with cell lysis buffer, and the protein concentration in each sample was adjusted to 25 μg/μl. The protein solutions were then incubated for 60 min in reaction buffer containing 7-amino-4-trifluoromethyl coumarin (AFC) conjugated to either DEVD (Asp-Glu-Val-Asp) as a substrate for caspase-3, IETD (Ile-Glu-Thr-Asp) for caspase-8, or LEHD (Leu-Glu-His-Asp) for caspase-9. It was then possible to measure the caspase activity using a VersaFluor fluorometer (Bio-Rad, Hercules, CA, USA) with a 379–401 nm excitation filter and a 505–515 nm emission filter. The data were expressed in terms of the levels of AFC fluorescence intensity.

Mitochondrial membrane potential

Changes in mitochondrial permeability lead to release of cytochrome c into the cytoplasm, and provide an indication of apoptosis via the mitochondrial pathway. This process was defined as measured by the change in the membrane potential. Loss of MMP was determined by a fluorescent cationic dye, 5,5′,6,6′-tetrachloro-1,1′,3,3′-tetraethylbenzamidazolocarbocyanine iodide (Mit-E-Ψ mitochondrial permeability detection kit; BIOMOL Research Laboratories, PA, USA). This fluorescent dye easily penetrates cells and aggregates (red fluorescence) into negatively charged healthy mitochondria. When the MMP collapses, the dye no longer accumulates inside the mitochondria and is thus distributed throughout the cell. When dispersed in this manner, the fluorescent dye assumes a monomeric form, which fluoresces green and results in decreased red fluorescence intensity [37]. The changes in the MMP of U251MG cells 20 h after PDT (0.2 J/cm^2; method described above; n = 4) and in the untreated cells used as a control (n = 4) were measured using a VersaFluor fluorometer (Bio-Rad) with a 485–495 nm excitation filter and a 585–595 nm emission filter. The data were expressed in terms of the levels of relative fluorescence units (RFU).

Mitochondrial cytochrome c release assay

The isolation of a highly enriched mitochondrial fraction from the cytosolic fraction of U251MG cells, including both the untreated cells used as the control (n = 5) and apoptotic cells 20 h after PDT (0.2 J/cm^2; method described above; n = 5) was carried out using a Mitochondria/cytosol fractionation kit (BioVision, Mountain View, USA). U251MG cells were centrifuged at 600 × g for 5 min at 4(C, resuspended in 10 ml of ice-cold PBS, and centrifuged at 600 × g for 5 min at 4°C. The cells were then resuspended in 1.0 ml of cytosol extraction buffer mix containing dithiothreitol and protease inhibitors, and were incubated on ice for 10 min. After this incubation, the cells were homogenized using a ultrasonic homogenizer (Taitec, Tokyo, Japan) under ice-cold conditions. The homogenate was centrifuged at 700 × g for 10 min at 4°C and the supernatant was centrifuged at 10,000 × g for 30 min at 4°C. Then, the supernatant was collected as the cytosolic fraction for a quantitative assay of cytochrome c. For this analysis, a cytochrome c ELISA kit was used according to the manufacturer's instructions (Chemicon International, Inc., Temecula, CA, USA).

Statistical methods

A Mann–Whitney *U* test was used to analyze differences in caspase activity, MMP, and mitochondrial cytochrome *c* release between the control cells and the cells after PDT. A *P*-value of less than 0.05 was considered to be statistically significant.

Results

Pp IX accumulation in lined human glioma cells incubated with 5-ALA

The intensity of PpIX fluorescence, measured by a flow cytometer, is shown in Fig. 1. The intensity of PpIX fluorescence was recognized in all three glioma lines tested, and this intensity reached a plateau at approximately 4 h following exposure of the cells to 5-ALA. The peak of PpIX accumulation in U118MG cells, which was the highest among all of the cell lines, reached two-and-a-half times higher than that in the U251MG cells, and four times higher than that in the U87MG cells.

Phototoxicity

The damage to U251MG cells was evaluated by scattergrams using a flow cytometer 24 h after the cells were subjected to PDT (Fig. 2). Untreated cells, cells exposed to light (1.0 J/cm^2) alone, and cells exposed to 5-ALA alone were still alive. However, when the cells were exposed to both 5-ALA and light, cell death occurred with increasing light dosage (Fig. 3).

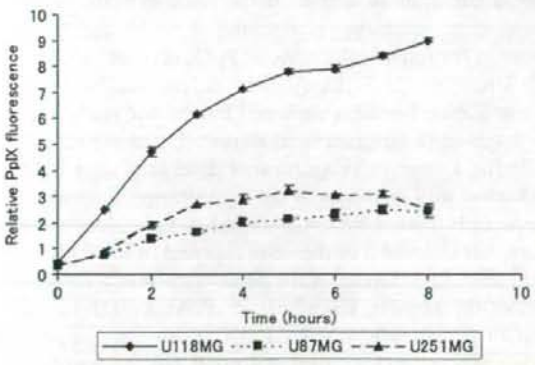

Fig. 1 PpIX accumulation in U251MG, U87MG, and U118MG cells incubated with 5-ALA. The intensity of PpIX fluorescence, measured by a flow cytometer, reached a plateau approximately 4 h after exposure of the cells to 5-ALA. PpIX accumulated in the highest amounts in U118MG cells. Data are based on three independent experiments. The data represent the mean ± SD

TUNEL staining

To analyze the cell death pathway, U251MG cells 24 h after PDT were assayed by the TUNEL staining method using a flow cytometer. The number of TUNEL-positive cells increased with light dosage after PDT (Fig. 4).

In the microphotographs of the TUNEL staining of U251MG cells 24 h after PDT (0.2 J/cm^2), a large number of apoptotic cells were observed (Fig. 5).

Caspase activity

The activities of caspase-3 and -9 were significantly elevated in U251MG cells after PDT ($P < 0.01$). However, the caspase-8 activity was not significant (Fig. 6). This result indicates that a mitochondrial pathway was mainly involved in the apoptosis induced by ALA-PDT in the U251MG cells.

Mitochondrial membrane potential

The non-apoptotic control cells gave off the bright red fluorescence of the fluorescent cationic dye in the mitochondria. However, in the cells subjected to PDT, this red fluorescence was not observed. This phenomenon is indicative of a decrease in the MMP. The levels of MMP were significantly decreased in U251MG cells after PDT ($P < 0.05$) (Fig. 7). This result demonstrated that changes in mitochondrial permeability led to the release of cytochrome *c* into the cytoplasm, and that these events occurred during the process of ALA-PDT.

Mitochondrial cytochrome c release

Cytochrome *c* in the cytosolic fraction was remarkably increased in the U251MG cells after PDT, as compared to the amount in the untreated cells ($P < 0.01$) (Fig. 8). The increment of cytochrome *c* in the cytosolic fraction demonstrated the release of cytochrome *c* from the mitochondria into the cytoplasm, which provided an initiation of apoptosis via a mitochondrial pathway.

Discussion

PDT is a promising local adjuvant therapy after surgery for patients with malignant gliomas. PDT involves the accumulation of a photosensitizing drug,

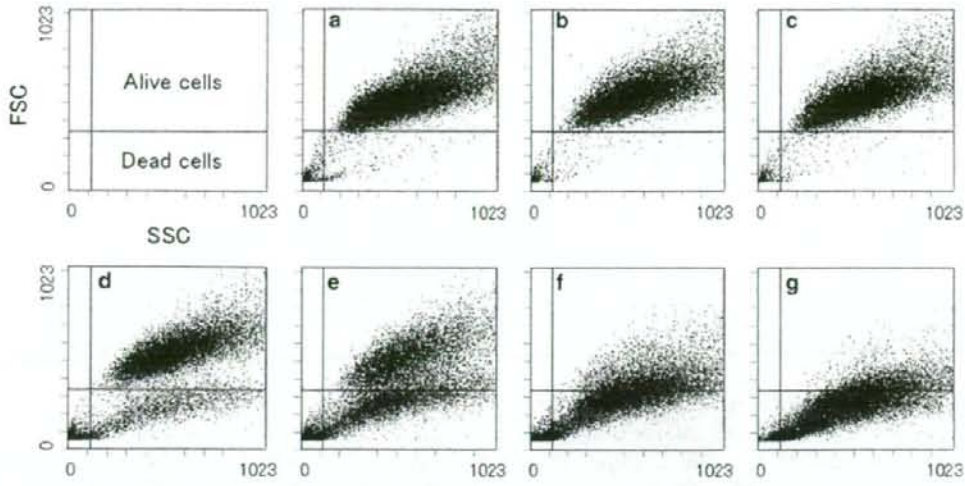

Fig. 2 Scattergrams of U251MG cells after PDT. Untreated cells (**a**), cells exposed to light (1.0 J/cm^2) alone (**b**), and cells exposed to 5-ALA alone (**c**) were still alive. However, when the cells were exposed to 5-ALA and light, dead cells were observed in numbers that were dependent on light dosages. (**d**) 0.1 J/cm^2, (**e**) 0.2 J/cm^2, (**f**) 0.5 J/cm^2, and (**g**) 1.0 J/cm^2. SSC = side scatter, FSC = forward scatter

preferentially in the tumor tissue, followed by irradiation of the cells with visible light of a specific wavelength [4]. Light activation of the photosensitizing drug induces the formation of reactive oxygen species such as singlet oxygen and hydroxyl radicals, which can cause severe cellular damage that leads to cell death [14, 29].

5-ALA is a naturally occurring metabolite that is a precursor to porphyrins in heme synthesis. Exogenous 5-ALA leads to the accumulation of the potent photosensitizer PpIX [19]. PpIX is known to accumulate more in malignant tissues than in normal tissues [10, 16, 19, 33]. ALA-PDT has been studied with promising results, especially for the treatment of skin and gastrointestinal malignancies [8, 9, 31, 32]. The benefits of ALA-PDT include easy administration and a short period of skin phototosensitization (1 or 2 days). Furthermore, 5-ALA shows excellent tumor-to-normal brain tissue localization [24, 38, 39, 40], such that it can selectively target residual infiltrating tumor cells in the peripheral cavity wall after glioma surgery.

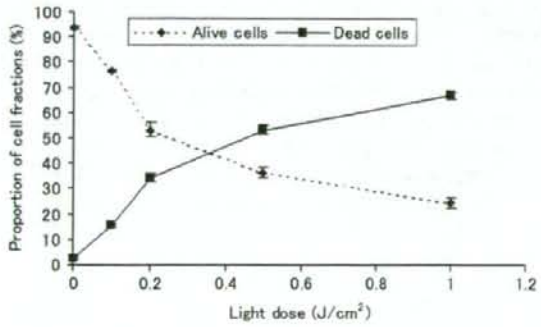

Fig. 3 Proportion of alive and dead fractions of U251MG cells after PDT as a function of light dose. This is a quantification of the results in Fig. 2. The proportion of dead cells increased with light dosage. The data represent the mean ± SD

The tumor-specific reduced activity of ferrochelatase, a rate-limiting enzyme in the last step of the heme biosynthesis pathway, is considered to be the main cause of the tumor selectivity of PpIX accumulation [5, 6]. Therefore, it is likely that differences in PpIX accumulation between each cell line in our study may be ascribed to differences in ferrochelatase activity.

In this study, the proportion of dead cells after PDT increased with increases in the light dosage. Almost all of the cells treated by 5-ALA alone or light alone were alive, but almost all of the cells exposed to PDT with a light dose of 1.0 J/cm^2 were dead. This result demonstrates the massive killing effect of ALA-PDT in the case of glioma cells in vitro. PpIX has the largest peak of the absorption spectrum at around 410 nm, and four peaks of the absorption spectrum occur between 500 nm and 650 nm [32]. Light at approximately 405 nm, as used in this study, was associated with the largest peak of the absorption spectrum of PpIX, and therefore this level may most efficiently induce cell

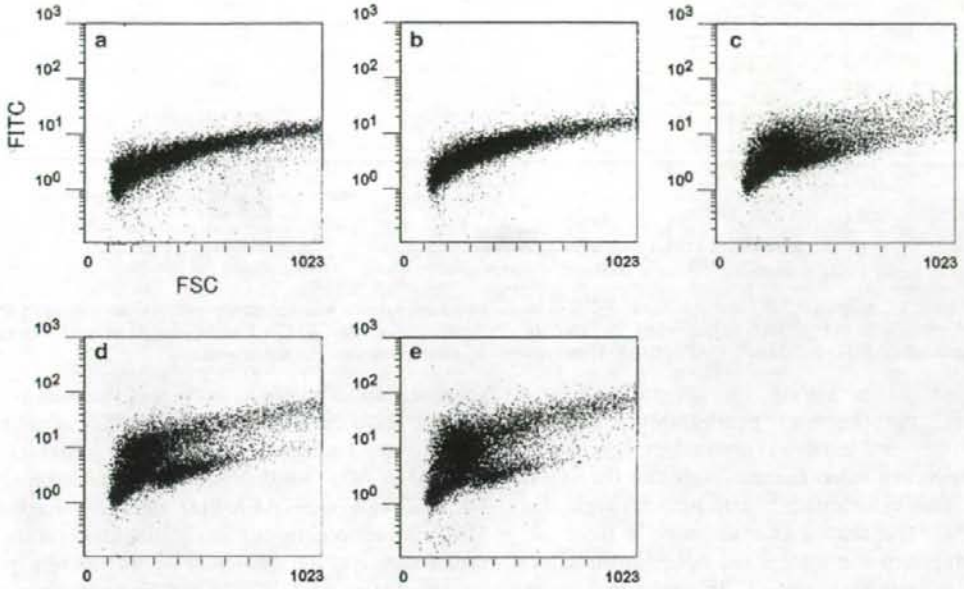

Fig. 4 TUNEL staining as evaluated by flow cytometric analysis. The number of TUNEL-positive cells increased with light dosage after PDT. (**a**) control, (**b**) 0.1 J/cm^2, (**c**) 0.2 J/cm^2, (**d**) 0.3 J/cm^2, and (**e**) 0.4 J/cm^2. Note the much higher number of TUNEL-positive cells in (**d**) and (**e**) than that observed in (**a**)

death. Taking in vivo treatment into consideration, there remains the problem that there is a limit to the lesion depth that can be reached by the light; thus, it may be necessary to use a longer wavelength of light (635 nm) together with the shorter wavelength [32]. Olzowy et al. [30] demonstrated that maximum phototoxic tissue reactions were observed to a depth of 3.7 mm in experiments using ALA-PDT with 635 nm of light and a Wistar rat C6 malignant glioma model. The depth observed in that study corresponded to the depth of this particular tumor, as demonstrated on pretreatment MR images. However, they concluded in that study that this value may not represent the limit of lesion depth achievable with 5-ALA, because experimental damage has also been perceived down to 7 mm and to 18 mm in the clinical setting with a hematoporphyrin derivative or Photofrin, the most optimal activation wavelength of which is 628 nm [17].

In this study, the number of TUNEL-positive cells increased with light dosage. It was therefore confirmed that the cell death pathway of U251MG cells after ALA-PDT was mainly apoptosis. Two pathways are currently considered to play major roles in regulating apoptosis. One of these pathways is mediated by death receptor/ligands, and the other is mediated by the mitochondria [15]. Procaspases 8 and 9 are activated by FADD in a Fas-mediated death receptor pathway, and by both cytochrome *c* and Apaf-1 in a mitochondrial pathway. Mitochondrial cytochrome *c* exists loosely attached in the mitochondrial intermembrane space.

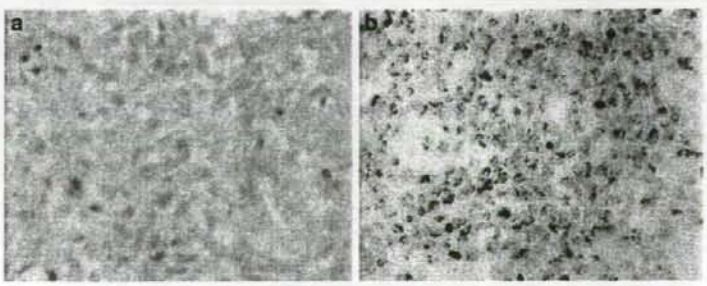

Fig. 5 TUNEL staining of cells after PDT (×200). Microphotographs of ALA-PDT (0.2 J/cm^2)-untreated (**a**) and ALA-PDT (0.2 J/cm^2)-treated (**b**) U251MG cells. TUNEL staining demonstrated numerous apoptotic cells after PDT

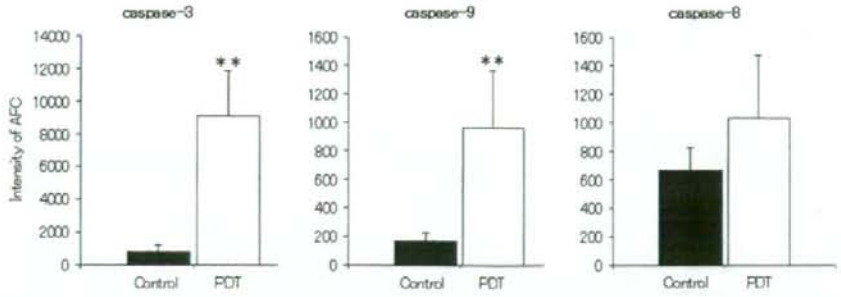

Fig. 6 Activities of caspase-3, -8, and -9 after PDT. The activities of caspase-3 and -9 were significantly elevated in U251MG cells after PDT (0.2 J/cm^2) (**$P < 0.01$). However, caspase-8 activity was not significantly elevated as compared to the control activity. AFC = 7-amino-4-trifluoromethyl coumarin. The data represent the mean ± SD

In response to a variety of apoptosis-inducing stimulations, mitochondrial permeability transition (PT) is induced. PT induces conformal changes in the voltage-dependent anion channel, such that the MMP decreases and cytochrome *c* can pass through the channel [41]. The release of cytochrome *c* from the mitochondria into the cytosol has been shown to be necessary to activate caspases. In the presence of dATP or ATP, cytochrome *c* binds to Apaf-1 and procaspase-9 [23, 43]. Caspase-9 is subsequently activated by the release of cytochrome *c* from the mitochondria, and this in turn leads to the activation of caspase-3 leads to cleavage of DNA repair enzymes and proteins with structural, signaling, or transcriptional function [3, 35]. It is generally thought that PDT with photosensitizers that localize in the mitochondria directly targets these mitochondria and causes both the rapid release of cytochrome *c* into the cytosol and caspase activation [2, 11, 20]. However, the signaling events resulting from ALA-PDT in glioma cells remained unclear until the findings of the present study clarified these events. Here, the activities of caspase-3 and -9 were significantly increased in U251MG cells after ALA-PDT. Furthermore, we demonstrated that U251MG cells after ALA-PDT showed a decrease in MMP. Moreover, in our study, the concentration of cytochrome *c* in the cytosolic fraction was remarkably increased after ALA-PDT. These findings, when taken together, render it reasonable to assume that a dysfunction in the MMP is followed by mitochondrial cytochrome *c* release, which in turn triggers apoptotic cell death through the mitochondrial pathway. Grebeňová et al. [12] reported that ALA-PDT in the leukemia cell line HL60 initiated several signaling process that led to rapidly progressing apoptosis, which was then followed by slow necrosis. Two apoptotic processes proceeded in parallel, one representing the mitochondrial pathway that was induced by the release of cytochrome *c* following the dysfunction of the MMP, and the other involving a disruption of calcium

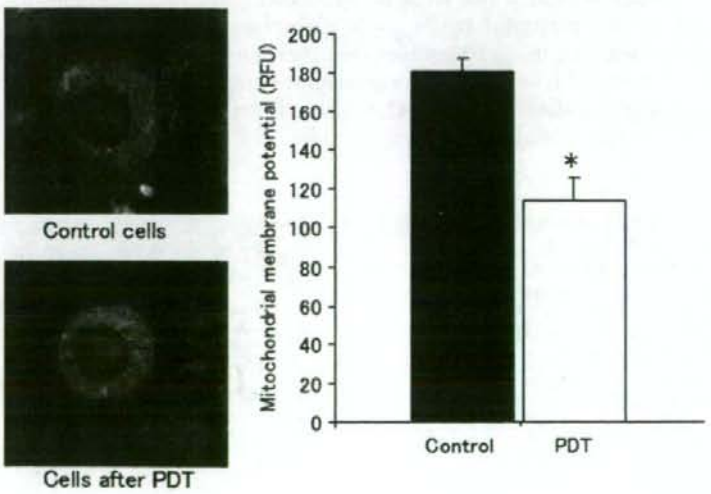

Fig. 7 Levels of mitochondrial membrane potential after PDT. Left column: Non-apoptotic control cells gave off bright red fluorescence from a fluorescent cationic dye in the mitochondria. However, cells treated with PDT, the red fluorescence was not observed. Right column: The decrease in the MMP. The MMP levels were significantly decreased in U251MG cells after PDT (0.2 J/cm^2) (*$P < 0.05$). The data represent the mean ± SD

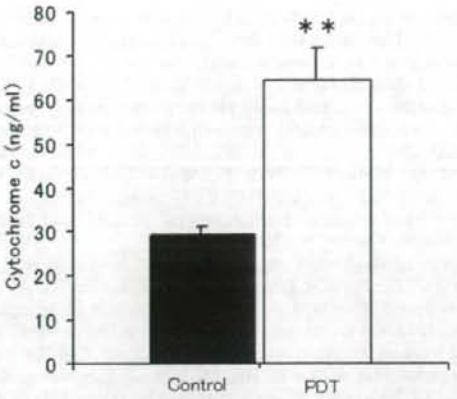

Fig. 8 Mitochondrial cytochrome *c* release after PDT. Cytochrome *c* in the cytosolic fraction was remarkably increased in U251MG cells after PDT (0.2 J/cm^2) (**$P < 0.01$). The data represent the mean ± SD

homeostasis and the activation of the endoplasmic reticulum stress-mediated pathway. Therefore, the latter pathway may play a role in the effectiveness of ALA-PDT in glioma cells; further investigation of this cell death mechanism will be necessary in the future.

In this study, a mitochondrial-pathway type of apoptosis, due to ALA-PDT, was confirmed in U251MG cells, which express endogenous mutant p53 [7]. The present findings indicate that this type of therapy is a strong initiator of apoptosis due to the direct activation of a mitochondrial pathway, independent of p53 status. This type of therapy appears to be applicable not only to apoptosis-sensitive tumors, but also to apoptosis-resistant neoplasms. As most malignant gliomas are well known to be chemo- and radio-resistant due to the inhibition of an apoptotic pathway, ALA-PDT may be suitable for the treatment of patients with a malignant glioma.

Conclusions

The present study revealed elevations in caspase-3 and -9 activity, a decrease in the MMP, and the release of cytochrome *c* from the mitochondria after ALA-PDT in U251MG cells. These results demonstrate that the cause of cell death after ALA-PDT in U251MG cells is mainly apoptosis via the mitochondrial pathway. Therefore, it is possible that ALA-PDT may be able to induce the apoptotic cell death of residual tumor cells in patients with chemo- and radio-resistant malignant gliomas. These results suggest that ALA-PDT may become a very useful local adjuvant therapy after the surgical resection of malignant gliomas.

Acknowledgment We would like to thank Teruo Ueno of the Central Research Laboratory at Osaka Medical College for his technical support with the flow cytometric analysis. Investment/Financial. Disclosure:This work was supported by Grants-in-Aid for Scientific Research (C) (14571345), (C) (15500351), and by a Grant-in-Aid for Exploratory Research (14657350) from the Japanese Ministry of Education, Science and Culture, awarded to Drs. T. Kuroiwa, Y. Kajimoto, and S. Miyatake, respectively. Additional support was provided in the form of a grant from the Promotion and Mutual Aid Corporation for Private Schools of Japan and the Science Research Promotion Fund to Dr. S. Miyatake and by a grant from the High-Tech Research Program of Osaka Medical College.

References

1. Agarwal ML, Clay ME, Harvey EJ, Antunez AR, Oleinick NL (1991) Photodynamic therapy induces rapid cell death by apoptosis in L5178Y mouse lymphoma cells. Cancer Res 51:5993–5996
2. Carthy CM, Granville DJ, Jiang H, Levy J, Rudin CM, Thompson CB, McManus BM, Hunt DWC (1999) Early release of mitochondrial cytochrome c and expression of mitochondrial epitope 7A6 with a porphyrin-derived photosensitizer: Bcl-2 and Bcl-xL overexpression do not prevent early mitochondrial events but still depress caspase activity. Lab Invest 79:953–965
3. Casciola-Rosen L, Nicholson DW, Chong T, Rowan KR, Thornberry NA, Miller DK, Rosen A (1996) Apopain/CPP32 cleaves proteins that are essential for cellular repair: a fundamental principle of apoptotic death. J Exp Med 183:1957–1964
4. Dougherty TJ, Gomer CJ, Henderson BW, Jori G, Kessel D, Korbelik M, Moan J, Peng Q (1998) Photodynamic therapy. J Natl Cancer I 90:889–900
5. El-Sharabasy MMH, El-Waseef AM, Hafez MM, Salim SA (1992) Porphyrin metabolism in some malignant disease. Br J Canc 65:409–412
6. Gibson SL, Cupriks DL, Havens JJ, Nguyen ML (1998) A regulatory role for porphobilinogen deaminase (PBGD) in δ-aminolevulinic acid (δ-ALA)-induced photosensitization. Br J Canc 77:235–243
7. Gomez-Manzano C, Fueyo J, Kyritsis AP, Steck PA, Roth JA, McDonnell TJ, Steck KD, Levin VA, Yung WK (1996) Adenovirus-mediated transfer of the p53 gene produces rapid and generalized death of human glioma cells via apoptosis. Cancer Res 56:694–699
8. Gossner L, May A, Sroka R, Stolte M, Hahn EG, Ell C (1999) Photodynamic destruction of high grade dysplasia and early carcinoma of the esophagus after the oral administration of 5-aminolevulinic acid. Cancer 15:1921–1928
9. Gossner L, Stolte M, Sroka R, Rick K, May A, Hahn EG, Ell C (1998) Photodynamic ablation of high-grade dysplasia and early cancer in Barrett's esophagus by means of 5-aminolevulinic acid. Gastroenterology 114:448–455
10. Grant WE, Hopper C, MacRobert AJ, Speight M, Bown SG (1993) Photodynamic therapy of oral cancer: photosensitization with systemic aminolevulinic acid. Lancet 342:147–148

11. Granville DJ, Carthy CM, Jiang H, Shore GC, McManus BM, Hunt DW (1998) Rapid cytochrome c release, activation of caspases 3, 6, 7 and 8 followed by Bap31 cleavage in HeLa cells treated with photodynamic therapy. FEBS Lett 437:5–10
12. Grebeňová D, Kuželová K, Smetana K, Pluskalová M, Cajthamlová H, Marinov I, Fuchs O, Souček J, Jarolím P, Hrkal Z (2003) Mitochondrial and endoplasmic reticulum stress-induced apoptotic pathways are activated by 5-aminolevulinic acid-based photodynamic therapy in HL60 leukemia cells. J Photochem Photobiol B 69:71–85
13. Green DR, Reed JC (1998) Mitochondria and apoptosis. Science 281:1309–1312
14. Henderson BW, Dougherty TJ (1992) How does photodynamic therapy work?. Photochem Photobiol 55:145–157
15. Hengartner MO (2000) The biochemistry of apoptosis. Nature 407:770–776
16. Iinuma S, Farshi SS, Ortel B, Hasan T (1994) A mechanistic study of cellular photodestruction with 5-aminolaevulinic acid-induced porphyrin. Br J Cancer 70:21–28
17. Kaye AH, Hill JS (1992) Photodynamic therapy of cerebral tumors. Neurosurg Q 1:233–258
18. Kaye AH, Morstyn G, Apuzzo MLJ (1988) Photoradiation therapy and its potential in the management of neurological tumours. J Neurosurg 69:1–14
19. Kennedy JC, Pottier RH (1992) Endogenous protoporphyrin IX: a clinical useful photosensitizer for photodynamic therapy. J Photochem Photobiol B 14:275–292
20. Kessel D, Luo Y (1999) Photodynamic therapy: a mitochondrial inducer of apoptosis. Cell Death Differ 6:28–35
21. Kostron H, Obwegesser A, Jacober R (1996) Photodynamic therapy in neurosurgery: a review. J Photochem Photobiol B 36:157–168
22. Kroemer G, Zamzami N, Susin SA (1997) Mitochondrial control of apoptosis. Immunol Today 18:44–51
23. Li P, Nijhawan D, Budihardjo I, Srinivasla SM, Ahmad M, Alnemri ES, Wang X (1997) Cytochrome c and dATP-dependent formation of Apaf-1/caspase-9 complex initiates an apoptotic protease cascade. Cell 91:479–489
24. Lilge L, Wilson BC (1998) Photodynamic therapy of intracranial tissues: a preclinical comparative study of four different photosensitizers. J Clin Laser Med Surg 16:81–92
25. Luo Y, Chang CK, Kessel D (1996) Rapid initiation of apoptosis by photodynamic therapy. Photochem Photobiol 63:528–534
26. Martins LM, Earnshaw WC (1997) Apoptosis: alive and kicking in 1997. Trends Cell Biol 7:111–114
27. Muller PJ, Wilson BC (1995) Photodynamic therapy for recurrent supratentorial gliomas. Semin Surg Oncol 11:346–354
28. Nicholson DW, Thornberry NA (1997) Caspases: killer proteases. Trends Biochem Sci 22:299–306
29. Oleinick NL, Evans HH (1998) The photobiology of photodynamic therapy: cellular targets and mechanisms. Radiat Res 150:146–156
30. Olzowy B, Hundt CS, Stocker S, Bise K, Reulen HJ, Stummer W (2002) Photoirradiation therapy of experimental malignant glioma with 5-aminolevulinic acid. J Neurosurg 97:970–976
31. Peng Q, Berg K, Moan J, Kongshaug M, Nesland JM (1997) 5-Aminolevulinic acid-based photodynamic therapy: principles and experimental research. Photochem Photobiol 65:235–251
32. Peng Q, Warloe T, Berg K, Moan J, Kongshaug M, Giercksky K-E, Nesland JM (1997) 5-aminolevulinic acid-based photodynamic therapy: clinical research and future challenges. Cancer 79:2282–2308
33. Regula J, MacRobert AJ, Gorchein A, Buonaccorsi GA, Thorpe SM, Spencer GM, Hatfield AR, Bown SG (1995) Photosensitization and photodynamic therapy of oesophageal, duodenal and colorectal tumors using 5-aminolevulinic acid induced protoporphyrin IX—a pilot study. Gut 36:67–75
34. Rosenthal MA, Kavar B, Hill JS, Morgan DJ, Nation RL, Stylli SS, Basser RL, Uren S, Geldard H, Green MD, Kahl SB, Kaye AH (2001) Phase I and pharmacokinetic study of photodynamic therapy for high-grade gliomas using a novel boronated porphyrin. J Clin Oncol 19:519–524
35. Schlegel J, Peters I, Orrenius S, Miller DK, Thornberry NA, Yamin TT, Nicholson DW (1996) CPP32/Apopain is a key interleukin 1b converting enzyme-like protease involved in Fas-mediated apoptosis. J Biol Chem 271:1841–1844
36. Shapiro WR, Green SB, Burger PC et al (1989) Randomized trial of three chemotherapy regimens and two radiotherapy regimens in postoperative treatment of malignant glioma. Brain Tumor Cooperative Group Trial 8001. J Neurosurg 71:1–9
37. Shibata M, Horiguchi T, Morimoto J, Otsuki Y (2003) Massive apoptotic cell death in chemically induced rat urinary bladder carcinomas following in situ HSVtk electrogene transfer. J Gene Med 5:219–231
38. Stummer W, Novotny A, Stepp H et al (2000) Fluorescence-guided resection of glioblastoma multiforme by using 5-aminolevulinic acid-induced porphyrins: a prospective study in 52 consecutive patients. J Neurosurg 93:1003–1013
39. Stummer W, Stocker S, Novotny A et al (1998) In vitro and in vivo porphyrin accumulation by C6 glioma cells after exposure to 5-aminolevulinic acid. J Photochem Photobiol B 45:160–169
40. Stummer W, Stocker S, Wagner S et al (1998) Intraoperative detection of malignant gliomas by 5-aminolevulinic acid-induced porphyrin fluorescence. Neurosurgery 42:518–526
41. Yang J, Liu X, Bhalla K, Kim CN, Ibrado AM, Cai J, Peng TI, Jones DP, Wang X (1997) Prevention of apoptosis by Bcl-2: release of cytochrome c from mitochondria blocked. Science 275:1129–1132
42. Zardi SI, Oleinick NL, Zain MT, Mukhtar H (1993) Apoptosis during photodynamic therapy-induced ablative RIF-1 tumors in C3H mice. Photochem Photobiol 58:771–776
43. Zou H, Li Y, Liu X, Wang X (1999) An APAF-1-cytochrome c multimeric complex is a functional apoptosome that activates procaspase-9. J Biol Chem 274:11549–11556

J Neurosurg 107:128–135, 2007

Antivasospastic and antiinflammatory effects of caspase inhibitor in experimental subarachnoid hemorrhage

Keiichi Iseda, M.D., Shigeki Ono, M.D., Keisuke Onoda, M.D., Motoyoshi Satoh, M.D., Hiroaki Manabe, M.D., Mitsuhisa Nishiguchi, M.D., Kenji Takahashi, M.D., Koji Tokunaga, M.D., Kenji Sugiu, M.D., and Isao Date, M.D.

Department of Neurological Surgery, Okayama University Graduate School of Medicine, Dentistry, and Pharmaceutical Sciences, Okayama, Japan

Object. Inflammation in the subarachnoid space and apoptosis of arterial endothelial cells have been implicated in the development of delayed cerebral vasospasm after subarachnoid hemorrhage (SAH). The authors investigated mechanisms of possible antivasospastic effects of *N*-benzyl-oxycarbonyl-Val-Ala-Asp-fluoromethylketone (Z-VAD-FMK), a caspase inhibitor that can inhibit both inflammatory and apoptotic systems, in animal models of SAH.

Methods. Rabbits were assigned to three groups of eight animals each and were subjected to SAH by injection of blood into the cisterna magna. The experiments were performed in the following groups: SAH only, SAH + vehicle, and SAH + Z-VAD-FMK. The Z-VAD-FMK (1 mg) or vehicle (5% dimethyl sulfoxide) was intrathecally administered before SAH induction. Diameters of the basilar artery (BA) were measured on angiograms obtained before and 2 days after SAH. The BA diameter on Day 2 was expressed as a percentage of that before SAH. Interleukin (IL)–1β in the cerebrospinal fluid (CSF) was examined using Western blotting, and brains were immunohistochemically examined for caspase-1 and IL-1β. In a separate experiment, 20 rats were subjected to SAH and their brains were immunohistochemically assessed for caspase-1, IL-1β, and macrophages.

Results. In rabbits, Z-VAD-FMK significantly attenuated cerebral vasospasm (the BA diameter on Day 2 in SAH-only, SAH + vehicle, and SAH + Z-VAD-FMK groups was 66.6 ± 3.2%, 66.3 ± 3.7%, and 82.6 ± 4.9% of baseline, respectively), and suppressed IL-1β release into the CSF and also suppressed immunoreactivities of caspase-1 and IL-1β in macrophages infiltrating into the subarachnoid space. Immunoreactivities for caspase-1 and IL-1β were observed in immunohistochemically proven infiltrating macrophages in rats.

Conclusions. These results indicate that caspase activation may be involved in the development of SAH-induced vasospasm through inflammatory reaction. *(DOI: 10.3171/JNS-07/07/0128)*

Key Words • caspase inhibitor • cerebral vasospasm • inflammation • macrophage • subarachnoid hemorrhage

Delayed cerebral vasospasm with subsequent cerebral ischemia, which usually develops approximately 1 week after SAH, is one of the major causes of morbidity and mortality in patients with ruptured cerebral aneurysms.[15] Despite numerous clinical and experimental studies, the pathophysiological mechanisms underlying cerebral vasospasm have yet to be fully elucidated, and one of the reasons for this is that this peculiar phenomenon seems to be multifactorial.[32] Inflammatory reaction in the subarachnoid space has long been considered to be one of the multiple causative factors.[1,11,16,19,25–28] Several lines of evidence have recently been found to support the suggestion that SAH may possibly cause arterial endothelial damage in an apoptotic fashion, eventually triggering or aggravating cerebral vasospasm.[35]

The caspase family is a group of cysteine proteases and has two major properties—as a regulator of proinflammatory and proapoptotic reactions.[18] Caspase-1 is a major proinflammatory caspase and directly converts immature IL-1β into its mature form and is implicated in various inflammatory responses.[6,7,33] Caspases such as 3, 8, and 9 play critical roles in the execution of apoptosis.[30] In this study, we used animal models of SAH to investigate mechanisms of a possible antivasospastic effect of an irreversible, broad-spectrum caspase inhibitor, Z-VAD-FMK, which can inhibit both inflammatory and apoptotic systems.

Abbreviations used in this paper: BA = basilar artery; CSF = cerebrospinal fluid; DMSO = dimethyl sulfoxide; IgG = immunoglobulin G; IL = interleukin; PBS = phosphate-buffered saline; SAH = subarachnoid hemorrhage; Z-VAD-FMK = *N*-benzyl-oxycarbonyl-Val-Ala-Asp-fluoromethylketone.

Materials and Methods

All procedures used in this study were performed according to the public health standards at Okayama University Graduate School of Medicine, Dentistry, and Pharmaceutical Sciences.